AIAA SciTech Forum
12-16 January 2026, Orlando, FL
AIAA SCITECH 2026 Forum

10.2514/6.2026-0815

Damping Modulation of Dampened Kapton Surfaces

Sebastian Esteban*, Jillian Wilson†
University of Central Florida, Orlando, Florida, USA

Emazuddin Alif‡, Andrew K. Dickerson§
University of Tennessee, Knoxville, Tennessee, USA

Jeffrey L. Kauffman¶
University of Central Florida, Orlando, Florida, USA

Vibrating droplets exhibit complex sloshing motion, an understudied behavior in drop physics. In general, sloshing involves a combination of droplet motion, deformation, and mass redistribution in all three dimensions. For microflyers in damp or wet environments, the dynamics of these drops on flight surfaces can significantly alter performance. As part of a larger project studying droplet adhesion and ejection on flexible, millimeter-scale wings, the current effort addresses the influence of a sloshing droplet on a highly flexible structural element inspired by insect wings. The ability of drops to deform and even relocate complicates the task of determining the dynamics of a microflyer wing. Our current understanding of sloshing stems from previous work on droplets of various viscosities placed at the end on the top surface of a cantilever beam. These experiments were repeated across a range of various beam thicknesses and demonstrated an influence that depended on the beam's excitation frequency. This paper investigates how the droplet viscosity and volume influence its fundamental sloshing natural frequency. Experiments revealed an inverse relationship between drop volume and natural frequency. Moreover, comparing drops with the same volume but different viscosity showed an additional inverse relationship between drop viscosity and natural frequency. In addition, increasing drop viscosity significantly increased the drop damping; i.e., drop free vibrations damped out much more quickly than in drops with lower viscosity.

Nomenclature

A	=	Vibration Amplitude
AR	=	Aspect Ratio
c	=	Damping
d	=	Maximum Width
F_i	=	Force
$F_{i,T}$	=	Force
$F_{\text{ad},N}$	=	Normal Adhesion Force
$F_{\text{ad},T}$	=	Tangential Adhesion Force
$F_{i,N}$	=	Normal Force
$F_{i,T}$	=	Tangential Force
f_n	=	Natural Frequency
g	=	Gravitational Acceleration
H	=	Droplet Height
h'	=	Distance
k	=	System Stiffness
m	=	Mass

*Undergraduate Research Assistant, Department of Mechanical and Aerospace Engineering, AIAA Student Member.
†Undergraduate Research Assistant, Department of Mechanical and Aerospace Engineering.
‡Graduate Research Assistant, Mechanical, Aerospace, and Biomedical Engineering Department.
§Associate Professor, Mechanical, Aerospace, and Biomedical Engineering Department.
¶Associate Professor, Department of Mechanical and Aerospace Engineering, AIAA Associate Fellow.

Oh = Ohnesorge Number
R = Nozzle Radius/Spherical Drop Radius
$\ddot{r}$ = Acceleration
V = Tip Velocity
Γ = Dimensionless Acceleration Amplitude
δ = Distance from droplet and cantilever surface
θ_e = Equilibrium Contact Angle
μ = Dynamic Viscosity
ρ = Density
σ = Surface Tension
ψ = Specific Damping Capacity
ω = Angular Frequency

I. Introduction

When a mosquito or similarly sized insect takes flight, a seemingly negligible small droplet will greatly hinder its flight performance. To ensure safe flight, mosquitoes conduct a low-amplitude, high-frequency, flutter-like motion to eject and decontaminate their wings of droplets and other particulates [1]. In contrast, mosquitoes wings in flight actuate with much greater amplitude but at much lower frequency. During both phases of wing motion, mosquitoes generate approximately 2,500 g of wing-tip acceleration, but with vastly different amplitude/frequency combinations corresponding to the different stroke objective: decontamination or flight. This study investigates the first part of a three-part research project focusing on systems exhibiting deformable solid dynamics that are highly dependent on coupled liquids. The droplet's behavior is investigated under free vibration to identify complex motion of liquid droplets. It is anticipated that planar solid motion and mass redistribution will be observed through the sloshing of droplets from free vibration. This research aims to identify an effective method to rapidly decontaminate small surfaces. The primary focus of this study is on how the natural frequency of a droplet is affected by the volume and viscosity of a droplet on a stationary surface. Having a better understanding of this frequency dependence will reveal new physics of temporal drop sloshing, fragmentation, and damping. For example, the effect of a solid mass on an actuated, flexible, cantilever beam can be modeled in a relatively straightforward fashion, at least for first-order effects. A sloshing droplet, however, may impart a dynamically varying level of inertia; moreover, it may relocate along the beam during vibration. All these effects will depend on relative droplet and beam size, droplet contents (e.g., density, viscosity), and the droplet-beam interface (e.g., wettability). This paper starts this analysis by revealing how a droplet on a rigid surface experiences free vibration; the hypothesis is that as the viscosity and volume of a disturbed stationary droplet increases, the droplet's natural frequency will decrease.

II. Background

The coupled fluid-structure interaction is not well studied in regard to drop physics. Gathering experimental and numerical data on this interaction can enable more accurate predictions of droplet behavior. Previous studies focused on how inertial loads relate to vehicle movement [2–6]. This includes the previously mentioned supercooled droplets causing significant performance loss when flying in certain environments[7]. This study departs from existing knowledge by focusing on multi-dimensional compliant substrates that do not have any kind of prescribed motion. Sloshing is a relatively understudied concept, as there is no standardized way to quantify "slosh." The droplet aspect ratio (AR) has been used in previous investigations to quantify droplet behavior using the equation

$$AR = \frac{H}{d} \tag{1}$$

where d is described as the maximum width of the droplet and H is the height of the elongated or flattened drop from the contact surface [8]. The droplet aspect ratio equation fails to capture the complex behavior of a sloshing droplet. The equation captures the movement of the droplet from its most elongated vertical point and its most elongated horizontal point which does not describe any of the internal movement or other smaller peaks as it is sloshing. The droplet's behavior can be extremely varied depending on the viscosity of the droplet, the material, and thickness of the cantilever, and the frequency of the vibrations that induce sloshing. Due to the nature of sloshing, there is a change in not only the transverse motion and weight of the droplet, but also the effective mass of the droplet which changes as the droplet

deforms vertically and changes the weight observed on the cantilever. Characterizing the sloshing motion as a response to structural vibration will assist in understanding the mechanics of droplet ejection. Achieving a better understanding of the self-decontamination approach may allow it to be implemented in the medical, scientific, aviation, etc. fields as decontamination is essential for surfaces like mosquito wings. This research focuses on the first part of a collaborative study between experts of experimental drop mechanics and damping dynamics. This research approach is inspired by the dynamical system mosquitoes use to decontaminate their wings, removing moisture prior to flight. Figure 1 shows the change in deflection during the flutter motion over time to quantitatively describe this three-step behavior. In this process, the mosquito starts with a flutter stroke, then moves into a transitional fluttering, and finally to a normal stroke that allows for the ejection of droplets and contaminants in a matter of milliseconds [1].

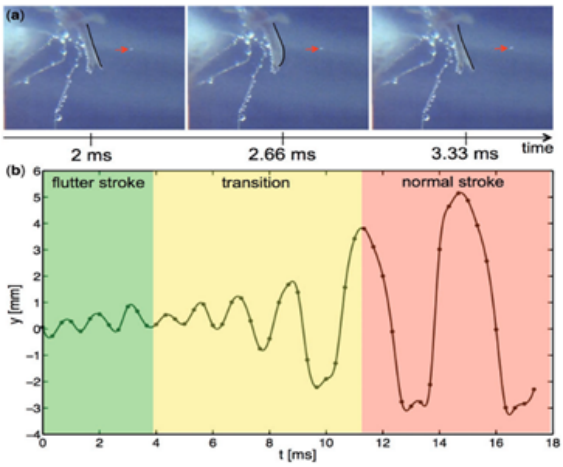

Fig. 1 The (a) photos show the mosquito in flutter stroke and ejecting the droplets. The (b) graph shows a quantitative representation of the deflection(mm) versus time(ms) throughout the flutter, transitional normal stroke.

Preliminary work investigated how droplets affects the damping of cantilevers with various droplet viscosities. This was done by determining the specific damping capacity, ψ [9], for the i^{th} cycle utilizing the equation

$$\psi_i = \frac{(V_i^2 - V_{i+1}^2)}{V_i^2} \tag{2}$$

where tip velocity V is measured at $y = 0$. Figure 2 shows a plot of ψ verses dimensionless acceleration amplitude, Γ for a 0.13mm cantilever. Γ is described as

$$\Gamma = \frac{A\omega^2}{g} \tag{3}$$

where A is the vibration amplitude, ω is the angular frequency, and g is the acceleration due to gravity. This is in order to find a viscosity that imposes the greatest damping.[9] The viscosity of the liquids are categorized utilizing the dimensionless Ohnesorge Number to describe the correlation between surface tension effects and viscosity. Ohnesorge Number is as

$$Oh = \frac{\mu}{\sqrt{\rho\sigma R}} \tag{4}$$

where μ is the dynamic viscosity of the liquid, ρ is the density, σ is the surface tension and R is the nozzle radius or the length [10]. The equation demonstrates that smaller, more viscous drops are more likely to eject as they are less prone to deformation with surfaces of lower adhesion [11]. These experiments demonstrate that changing surface tension has minimal effect on damping, but a large effect on drop shape (inertial load) [9]. Understanding the drop shapes at a more fundamental level requires exploring water droplet movement outside of prescribed motion. The natural frequency of a disturbed water droplet gives insights into the dynamics of a water droplet sloshing motion. Natural frequency is determined through its stiffness and mass, which are the properties of a free dynamical system

$$f_n = \frac{1}{2\pi}\sqrt{\frac{k}{m}} \tag{5}$$

where f_n is the natural frequency, k is the system's stiffness, and m is the mass of the system. The natural frequency of a system of droplets gives us insight into the behavior acting within the droplet by exploring how the mass and stiffness of a complex system, such as a droplet sloshing, interact with each other [12]. This study builds upon this preliminary work by performing similar experiments with droplets on cantilevers of variable thickness.

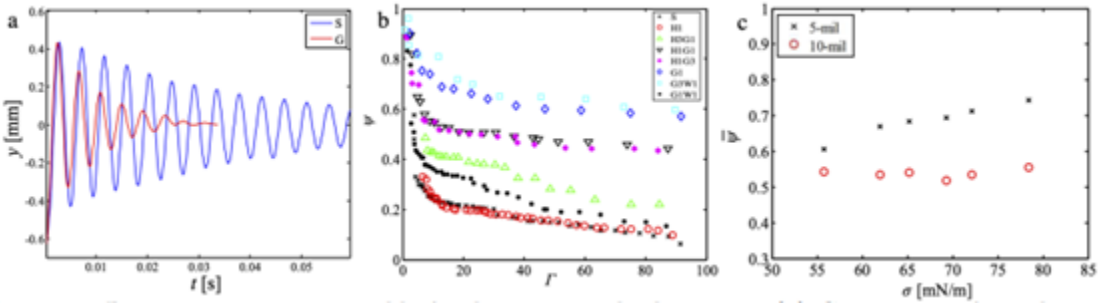

Fig. 2 Damping tip displacement is occurs due to drop viscosity. (a) Comparison of cantilever tip displacement with solid (S) and glycerin (G1) masses. (b) Specific damping capacity ψ versus ejective acceleration for a 0.13-mm cantilever top with liquids of various viscosity. (c) Average damping capacity ψ for changing surface tension of a mixed glycerin-water drop.

Previous works display the complexity of the unsteady inertial loads by focusing on drop properties, cantilever motion, and cantilever wetting properties that identify a particular ejection mode where the base motion amplitude is fixed, and attempts to quantify the dampening induced by sloshing sets the groundwork for this research [13]. The kinematic assumption provided by Euler-Bernoulli Beam Theory and small deflections would under normal circumstances describe the interactions from equilibrium to the equation of motion. The added variable of larger deflections of the droplet, which provides a new theoretical point mass, keeps us from using the aforementioned assumption [14]. Y. Chen's extension of Hamilton's Principle develops the methodology for describing the dynamic system in a motion equation [15]. Applying the assumed-modes method with von Kármán strains to model the large deflection of the thin beam results in the nonlinear form.

$$M\ddot{a} + c\dot{a} + k_L a + k_{NL} a^3 = -M_0 \ddot{a}_0(t) \tag{6}$$

where $a(t)$ is the function describing the amplitude of the assumed mode motion; a_0 represents beam/drop system's base motion of the beam/drop system. The linear equivalent mass, damping, and stiffness variables are M, c, and k, respectively. k_{NL} is the term that shows how the beam bends and moves nonlinearly. M_0 is the term that represents an integration of deformable motions and the rigid base of the drop/beam system. [16] Using Hamilton's principle, the stiffness and mass variables can be directly calculated from energy and work. The damping terms selection is influenced by the application, as boundary conditions have a considerable impact on energy dissipation [15, 17–21]. Despite our understanding of Hamilton's principle, one of the current struggles of understanding the motion of cantilevers in the context of drops of liquid is drop inertia. Previous research has investigated how time-dependent inertial factors affect a structure, but a liquid drop's deformation is unpredictable because as the droplet sloshes, its effective weight and mass distribution change, which develops liquid accelerations that can vary greatly [3].

The center of mass of the drop on a cantilever at rest uses x_0 as the distance from base and from the cantilever surface the distance is represented by δ which will make angle $w'(x_0, t)$ with respect to the horizontal axis which is represented in Figure 3. Newton's Second Law describes the force that is acting on a steady drop's center of inertia the center of mass of a drop on a cantilever at rest

$$F_i = m_{\text{drop}} \ddot{r} \tag{7}$$

Here the position vector r describes the location of the drop on the cantilever. Assuming a spherical curvature of the drop, the drop mass is described as

$$m_{\text{drop}} = \rho\pi \left[\frac{4}{3} R^3 - R^2 h' + \frac{(h')^2}{3} - (h')^2 \cos\theta_e + R^2 h' \cos^2\theta_e \right] \tag{8}$$

where R is the spherical drop radius, the equilibrium contact angle is θ, and h' is the distance the sphere would protrude below the cantilever [8].

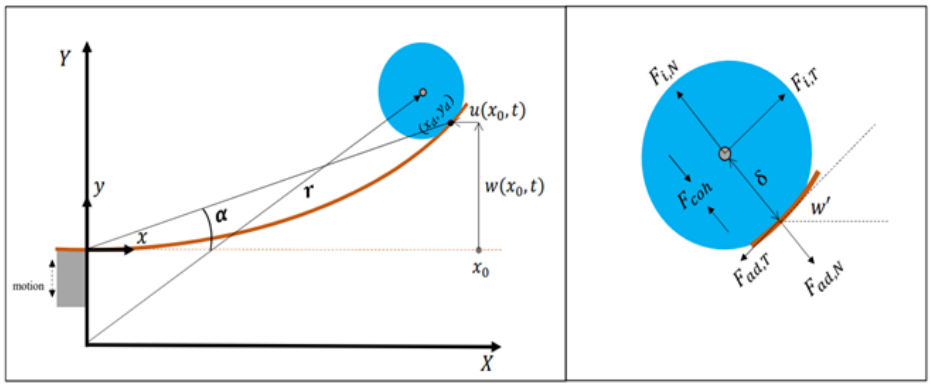

Fig. 3 A free-body diagram of a liquid drop on a cantilever under deflection.

Using Newton's Second Law, we can define the normal and tangential forces,

$$F_{i,T} = m_{\text{drop}}\, \ddot{r}^{*}(\cos\omega'\,\hat{i} + \sin\omega'\,\hat{j}) \tag{9}$$

$$F_{i,N} = m_{\text{drop}}\, \ddot{r}^{*}(-\sin\omega'\,\hat{i} + \cos\omega'\,\hat{j}) \tag{10}$$

the adhesion force is also represented through components $F_{\text{ad},T}$ and $F_{\text{ad},N}$ in the equations.

$$F_{\text{ad},T} = k_s R\sigma(\cos\theta_r - \cos\theta_a) \tag{11}$$

Although we attempt to explore and quantify the movement of the droplet in the system through $F_{\text{ad},T}$ and $F_{\text{ad},N}$, there is no current existing closed-form solution for the cohesive force that keeps the drops intact for sloshing, deforming drops [22].

III. Methodology

Unlike preliminary experimentation, this investigation investigates the droplet on a flat surface. A 15.24-mm by 3.81-mm piece of Kapton is secured on a flat elevated position, which, for our purposes, was a piece of Kapton taped to a table that was level with the camera. This portion of the experiment tests the volume and viscosity of the droplet in relation to its natural frequency.

The corner of a separate piece of Kapton is used to then disturb the water droplet by placing the corner tip of the Kapton piece onto the water droplet and then quickly lifting the Kapton sheet upwards. The reactionary sloshing is

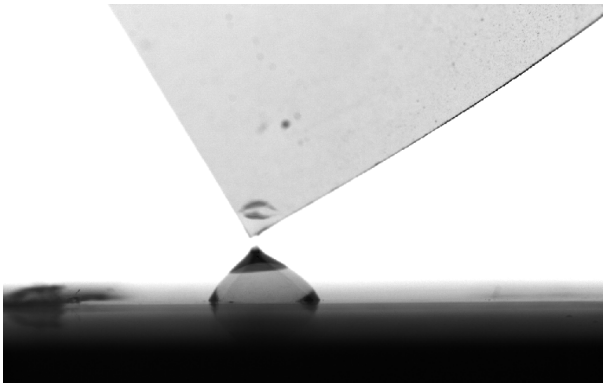

(a) An 11-μL droplet just after an has been disturbed.

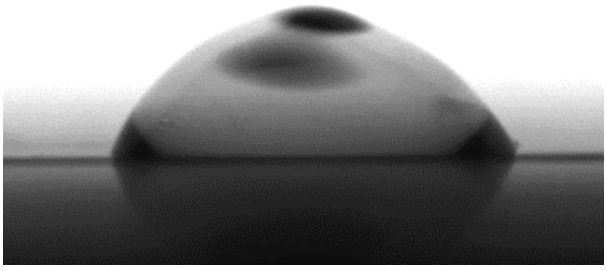

(b) An 11-μL droplet sloshing after being disturbed.

Fig. 4 Direct disturbance generated free vibration droplet motion.

observed and recorded. This experiment includes the reactions of both water and a 75% glycerin-water solution at 1, 3, 5, 7, 9, and 11 μL, with 5 recordings for each.

The high-speed videography is taken using a Fastcam Mini AX 200 camera utilizing a Sigma 105-mm lens on a tripod, capturing at 6400 fps and 512 x 384 resolution. As a backdrop for the footage of the cantilever, a Neewer background light is set at 5600 K to isolate and emphasize the droplet and its behavior during filming. To observe and record the camera footage, the Photron Fastcam Viewer 4 (PFV4) program is run and utilized on one of the laboratory computers.

Captures of preliminary experiments shown in Figure 4b shows what is expected to be recorded during experimentation. The recording is cropped using ImageJ to reveal exclusively the beam and the droplet to optimize the analysis. The recordings are then cropped using the ImageJ software so just the droplet and its disturbance are visible in the recording. After binarization, the data creates an amplitude over time graph, then run through a Fast Fourier Transform (FFT) to find the natural frequency, which is then recorded to find the mean natural frequency for each case.

IV. Findings

For every experiment conducted, a single-sided amplitude spectrum graph is analyzed for the natural frequency, which is then compiled into the data points used for the results.

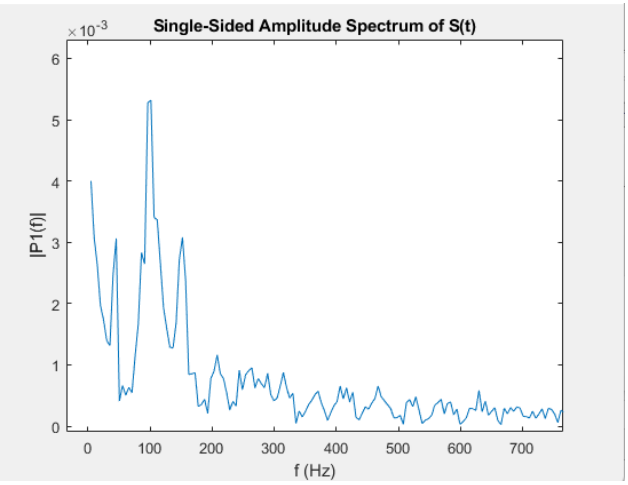

Fig. 5 Frequency graph from an 11-μL water droplet.

Figure 5 shows the peak of the graph that represents the natural frequency for the droplet. That peak value is then recorded and analyzed with the other trials in the test case. Analysis of the stationary water droplet experiments reveals an overall trend revealing an inverse relationship between water droplet volume and natural frequency.

Figures 6 and 7 show the general trend of the natural frequency decreasing as the volume of the droplet increases. Significant spread of the data points is observed for each volume case. Many cases such as the 5 μL has equal or less value for the natural frequency than the 7 μL.

When comparing the natural frequency of glycerin and a water drop of the same volume, indicating how the increase in viscosity leads to a decrease in the natural frequency for all the corresponding volumes. This is observed in Figure 8. It is important to note that the general spread of the glycerin values overlapped at times with the water droplet values such as the test cases for 5 μL and 11 μL.

V. Discussion

The equation for natural frequency describes the behavior of the stationary droplet, as the increase in overall rigidity from an increase in viscosity allows for a higher natural frequency. Despite this, a decrease in natural frequency is observed from the glycerin to its corresponding water counterpart. The inverse relationship between mass and natural frequency indicates that an increase in volume leads to a corresponding decrease in natural frequency. This is consistent between water and glycerin. Figures 6 and 7 showcase a substantial spread of values for many test cases. It is observed that certain volume test cases have trials where droplets of a lesser volume have a greater natural frequency. The current

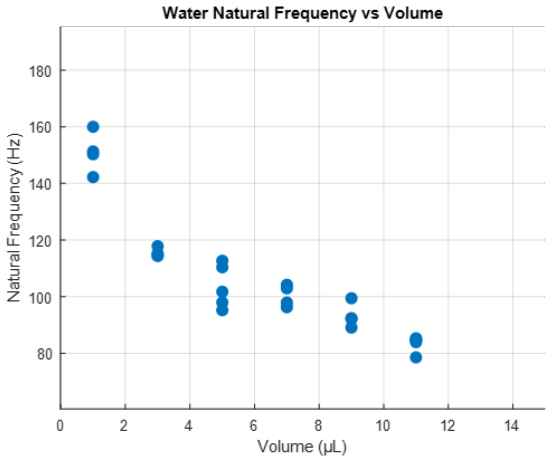

Fig. 6 Data plot for the water droplet experiments.

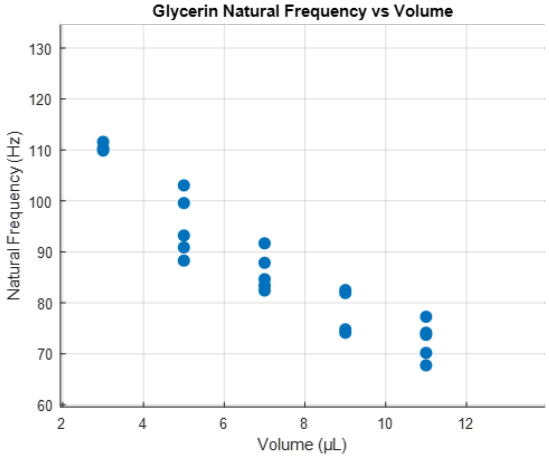

Fig. 7 Data plot for the glycerin droplet experiments.

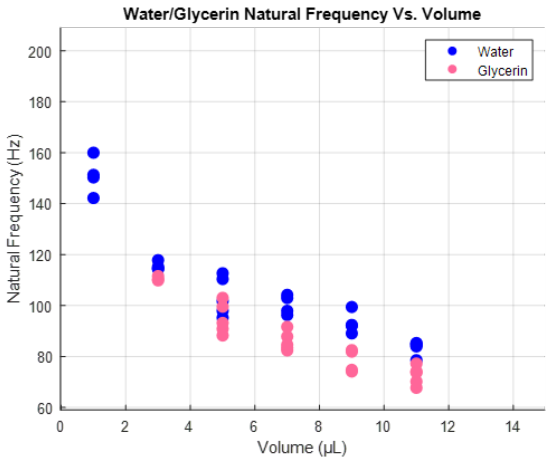

Fig. 8 The combination of water and glycerin values

hypothesis is that there is either an inconsistency of behavior of the droplet when disturbed or inconsistencies of the analysis code as the droplet is tracking the droplet's movement. The data presents a small portion of tests that were unreadable by the MATLAB analysis code, which provided unintelligible data or no data at all, despite no clear reason being observed from the recordings. These tests were redone with the same parameters. Seen in Figure 7, the testing cases for 1 μL are empty, as all original and subsequent captures failed to provide data or the data is intelligible. The subtlety of the vibration of the droplet likely made it difficult for the analysis code to provide unintelligible data. These outliers were recorded but not added within the values that were used to calculate the mean for each respective volume.

VI. Conclusion

This investigation sought to observe the practical effects that volume and viscosity have on the natural frequency of a liquid droplet when placed on a Kapton surface. Experiments show a general trend of a decrease in natural frequency as the liquid volume and viscosity increases for the droplet vibrating on a rigid surface. The relationships and trends observed present a new avenue for experimentation to validate and develop this investigation. Future investigations will consider additional viscosities, for example different water/glycerin mixtures to extend these trends. In addition, we anticipate studying different droplet-beam interfaces properties, for example using surfaces that have greater or lesser wettability than plain Kapton. We observed that water would remain on the Kapton "disturbance" sheet after disturbing the droplet. Although seemingly negligible, the water droplet will be slightly less than its assigned volume. Developing a method to keep the amount of water lifted out of the droplet proportional would keep the results more consistent in relation to each other. This effect will be more significant as the beam wettability decreases. In the limit of a highly hydrophobic surface, the droplet may simply adhere to the material used to disturb it. For these reasons, we also are investigating other methods to generate an initial droplet deformation, such as blowing a thin stream of air onto the droplet.

Acknowledgments

This work was sponsored by the National Science Foundation, administered through the NSF Division of Chemical, Bioengineering, Environmental, and Transport Systems (Award No. 2346687).

References

[1] Dickerson, A. K., and Hu, D. L., "Mosquitoes Actively Remove Drops Deposited by Fog and Dew," *Integrative and Comparative Biology*, Vol. 54, No. 6, 2014, pp. 1008–1013. URL `https://www.jstor.org/stable/26369801`, accessed 1 Apr 2025.

[2] Lee, H. P., "Transverse vibration of a Timoshenko beam acted on by an accelerating mass," *Applied Acoustics*, Vol. 47, 1996, pp. 319–330. https://doi.org/10.1016/0003-682X(95)00067-J.

[3] Michaltsos, G., Sophianopoulos, D., and Kounadis, A., "The effect of a moving mass and other parameters on the dynamic response of a simply supported beam," *Journal of Sound and Vibration*, Vol. 191, 1996, pp. 357–362. https://doi.org/10.1006/jsvi.1996.0127.

[4] Gutierrez, R. H., and Laura, P. A. A., "Vibrations of a beam of non-uniform cross-section traversed by a time varying concentrated force," *Journal of Sound and Vibration*, Vol. 207, 1997, pp. 419–425. https://doi.org/10.1006/jsvi.1997.1164.

[5] Zheng, D. Y., Cheung, Y. K., Au, F. T. K., and Cheng, Y. S., "Vibration of multi-span non-uniform beams under moving loads by using modified beam vibration functions," *Journal of Sound and Vibration*, Vol. 212, 1998, pp. 455–467. https://doi.org/10.1006/jsvi.1997.1435.

[6] Wang, Y. J., Shi, J., and Xia, Y., "Dynamic responses of an elastic beam moving over a simple beam using modal superposition method," *Journal of Vibroengineering*, Vol. 14, 2012, pp. 1824–1832.

[7] Politovich, M. K., "Aircraft Icing Caused by Large Supercooled Droplets," *Journal of Applied Meteorology and Climatology*, Vol. 28, No. 9, 1989, pp. 856 – 868. https://doi.org/10.1175/1520-0450(1989)028<0856:AICBLS>2.0.CO;2, URL https://journals.ametsoc.org/view/journals/apme/28/9/1520-0450_1989_028_0856_aicbls_2_0_co_2.xml.

[8] Ijavi, M., Style, R. W., Emmanouilidis, L., Kumar, A., Meier, S. M., Torzynski, A. L., Allain, F. H. T., Barral, Y., Steinmetz, M. O., and Dufresne, E. R., "Surface tensiometry of phase separated protein and polymer droplets by the sessile drop method," *Soft Matter*, 2021, pp. 1655–1662. https://doi.org/10.1039/D0SM01319F.

[9] Anonymous, "Personal Correspondence," Private communication, 2025.

[10] Radhakrishna, V., Shang, W., Yao, L., Chen, J., and Sojka, P. E., "Experimental characterization of secondary atomization at high Ohnesorge numbers," *International Journal of Multiphase Flow*, Vol. 138, 2021, p. 103591. https://doi.org/10.1016/j.ijmultiphaseflow.2021.103591.

[11] Tai, J., Gan, H. Y., Liang, Y. N., and Lok, B. K., "Control of Droplet Formation in Inkjet Printing Using Ohnesorge Number," *10th Electronics Packaging Technology Conference*, Singapore, 2008, pp. 761–766. https://doi.org/10.1109/EPTC.2008.4763524.

[12] Thomson, W. T., and Dahleh, M. D., *Theory of Vibrations with Applications*, 5th ed., Prentice Hall, Upper Saddle River, 1997.

[13] Alam, M. E., Kauffman, J. L., and Dickerson, A. K., "Drop ejection from vibrating damped, dampened wings," *Soft Matter*, Vol. 16, 2020, pp. 1931–1940.

[14] Stanton, S. C., Erturk, A., Mann, B. P., Dowell, E. H., and Inman, D. J., "Nonlinear nonconservative behavior and modeling of piezoelectric energy harvesters including proof mass effects," *Journal of Intelligent Material Systems and Structures*, Vol. 23, 2012, pp. 183–199. https://doi.org/10.1177/1045389X11432656.

[15] Chen, Y.-H., and Sheu, J.-T., "Axially-loaded damped Timoshenko beam on viscoelastic foundation," *International Journal for Numerical Methods in Engineering*, Vol. 36, 1993, pp. 1013–1027. https://doi.org/10.1002/nme.1620360609.

[16] Meirovitch, L., *Principles and Techniques of Vibrations*, Prentice Hall, Upper Saddle River, NJ, 1997.

[17] MacBain, J. C., and Genin, J., "Energy dissipation of a vibrating Timoshenko beam considering support and material damping," *International Journal of Mechanical Sciences*, Vol. 17, 1975, pp. 255–265. https://doi.org/10.1016/0020-7403(75)90007-7.

[18] Lundén, R., and Åkesson, B., "Damped second-order Rayleigh–Timoshenko beam vibration in space – an exact complex dynamic member stiffness matrix," *International Journal for Numerical Methods in Engineering*, Vol. 19, 1983, pp. 431–449. https://doi.org/10.1002/nme.1620190310.

[19] Xu, G. Q., and Yung, S. P., "Exponential decay rate for a Timoshenko beam with boundary damping," *Journal of Optimization Theory and Applications*, Vol. 123, 2004, pp. 669–693. https://doi.org/10.1007/s10957-004-5728-x.

[20] Lee, H.-L., and Chang, W.-J., "Effects of damping on the vibration frequency of atomic force microscope cantilevers using the Timoshenko beam model," *Japanese Journal of Applied Physics*, Vol. 48, 2009, p. 065005. https://doi.org/10.1143/JJAP.48.065005.

[21] Chen, W.-R., "Bending vibration of axially loaded Timoshenko beams with locally distributed Kelvin–Voigt damping," *Journal of Sound and Vibration*, Vol. 330, 2011, pp. 3040–3056. https://doi.org/10.1016/j.jsv.2011.01.015.

[22] Chini, S. F., Bertola, V., and Amirfazli, A., "A methodology to determine the adhesion force of arbitrarily shaped drops with convex contact lines," *Colloids and Surfaces A: Physicochemical and Engineering Aspects*, Vol. 436, 2013, pp. 425–433.